Evolution of the plastic zone near a microfracture: a numerical simulation and its implications on in situ stress measurement

YARLONG WANG[1]

Department of Civil Engineering, The University of Alberta, Edmonton, AB T6G 2G1, Canada

SAMUEL S. SHEN

Department of Mathematics, The University of Alberta, Edmonton, AB T6G 2G1, Canada

AND

HAIBING CHENG

Department of Civil Engineering, University of Waterloo, Waterloo, ON N2L 3G1, Canada

Received May 5, 1993

Accepted June 2, 1994

The instantaneous shut-in pressure has been used to estimate the far-field in situ minimum principal stress during microfracture testing. A plastic zone can be induced near the fracture. Because of the early plastic (irreversible) deformation induced near the fracture, the irreversible deformation near the fracture surface reduces the fracture pressure and generates a discrepancy between the far-field minimum stress and the fracture closure pressure, which has been identified as the minimum in situ stress in the past. In this paper, a finite-element numerical model is used to investigate this discrepancy due to the plastic deformation near a fracture. It is concluded that a plastic zone can be generated near a hydraulic fracture in poorly consolidated media. The fracture closure pressure can be much smaller than the minimum in situ stress due to the irreversible deformation generated near the fracture during the active fracturing period. Thus, one cannot use the conventional hydraulic-fracturing technique to interpret the minifracture tests in a poorly consolidated medium such as oil sand.

Key words: microfracturing, in situ stress measurements, oil sands, plasticity, numerical simulation.

La pression de fermeture instantanée a été utilisée au cours d'essais de microfracture pour évaluer la contrainte principale minimum in situ dans un massif. Une zone plastique peut être induite près de la fracture. Par suite de la déformation plastique (irréversible) précoce induite près de la fracture, la déformation irréversible près de la surface de la fracture réduit la pression de fracturation et produit une inconsistance entre la contrainte minimum dans le massif et la pression de fermeture de la fracture, qui a été identifiée comme étant la contrainte minimum in situ dans le passé. Dans cet article, un modèle numérique en éléments finis est utilisé pour étudier l'inconsistance due à la déformation plastique près de la fracture. L'on conclut qu'une zone plastique peut être générée près d'une fracture hydraulique dans un milieu faiblement consolidé. La pression de fermeture de la fracture peut être beaucoup plus faible que la contrainte minimum in situ à cause de la déformation irréversible générée près de la fracture durant la période active de fracturation. Ainsi, l'on ne peut pas utiliser la technique conventionnelle de fracturation hydraulique pour interpréter les essais de minifracturation dans un milieu faiblement consolidé tel que le sable bitumineux.

Mots clés : microfracture, mesures de la contrainte in situ, sables bitumineux, plasticité, simulation numérique.

[Traduit par la rédaction]

Can. Geotech. J. **31**, 779–787 (1994)

Introduction

The use of microfracture tests to determine in situ stress profiles has become a standard part of the hydraulic-fracturing treatment and design process. A conventional microfracture test consists of several consecutive short pumping cycles (usually 3–5) to pressurize a preselected interval of the well so that the adjacent rock formation may be fractured. Each cycle is followed by a shut-in period of about 15–20 min (Nolte 1979; Gronseth and Kry 1983; Boone et al. 1991*a*). A typical schematic pressure–time record is given in Fig. 1.

During the microfracture tests under our consideration, the pump was shut off once the fracture was opened. The pressure that had built up due to the pumping process declined rapidly because of the fluid dissipation into the rock formation and backflow of the fluid into the wellbore. The fracture continued to propagate after shut-in, and the fracture ultimately closed (Boone et al. 1991*a*). Conventionally, it is assumed that right at the moment of the fracture closure the pressure inside the fracture is equal to or slightly higher than the far-field stress normal to the fracture. Hence the minimum in situ stress in hard-rock regions can be estimated from the instantaneous shut-in pressure, extracted from the post-shut-in pressure curves obtained from the fracturing test (Nolte 1979; Gronseth and Kry 1983; Boone et al. 1991*a*).

Conventionally, the minimum in situ stress σ_h has been evaluated by

$$[1] \quad \sigma_h = p_s - \Delta\sigma$$

where p_s is the shut-in pressure, and $\Delta\sigma$ is the induced stress on the fracture surface, which is assumed to be negligible according to the conventional stress-measurement theory. Many factors, however, can make significant contributions to the induced stress $\Delta\sigma$, including the poroelastic effect (Boone 1989; Boone et al. 1991*b*) and the plastic deformation; the latter is subjected to study in this paper.

[1]Present address: Shell Canada Ltd., P.O. Box 2506, Calgary, AB T2P 3S6, Canada.

Printed in Canada / Imprimé au Canada

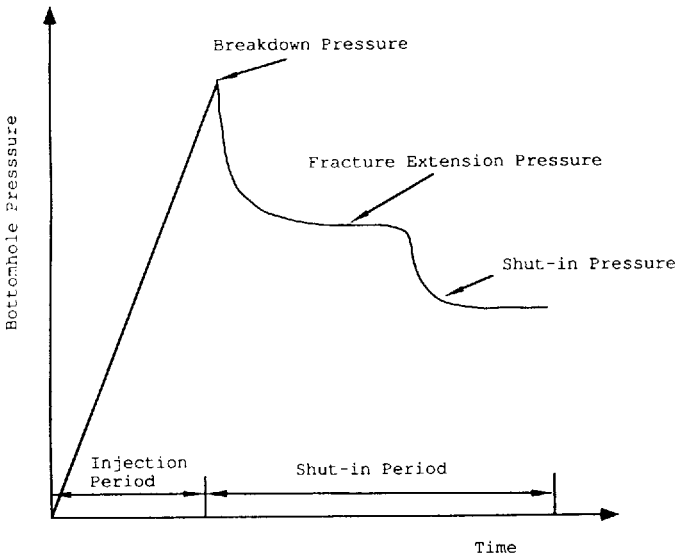

FIG. 1. A schematic diagram of a typical pressure–time curve for a microfracture test.

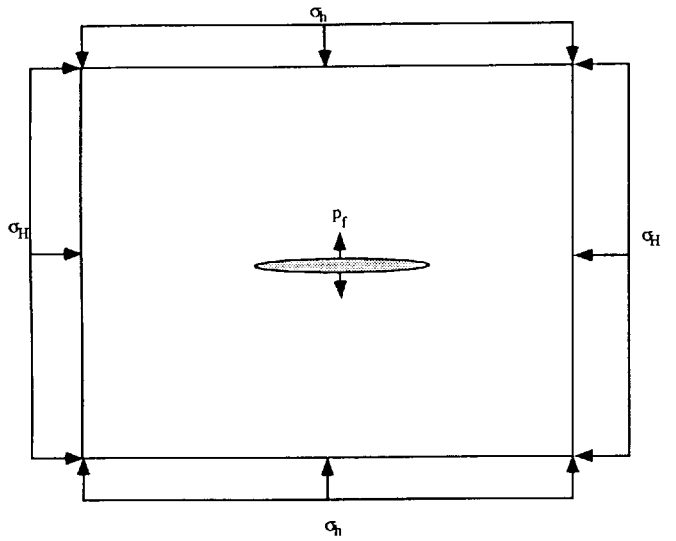

FIG. 2. A schematic diagram of a hydraulic fracture.

Once the minimum in situ stress σ_h is measured, the maximum in situ stress σ_H can be estimated using the following equation (Hubbert and Willis 1957; Haimson and Fairhurst 1969):

$$[2]\quad \sigma_H = 3\sigma_h - P_b + T_0 - P_0$$

where

P_b is the maximum bottom-hole pressure (i.e., breakdown or initiation),

P_0 is the virgin pore pressure, and

T_0 is the apparent tensile strength of the rock.

A large number of field data sets and experimental tests support this assumption (Haimson and Fairhurst 1969; Schmitt and Zoback 1989; Boone et al. 1991*a*). Yet the applicability of the theory to poorly consolidated rocks has neither been analyzed nor fully understood. The purpose of this paper is to address this issue. In the following, an elastic – perfectly plastic model is used to simulate a poorly consolidated medium. The elastic domain for the material under consideration is assumed to be bounded by a linear

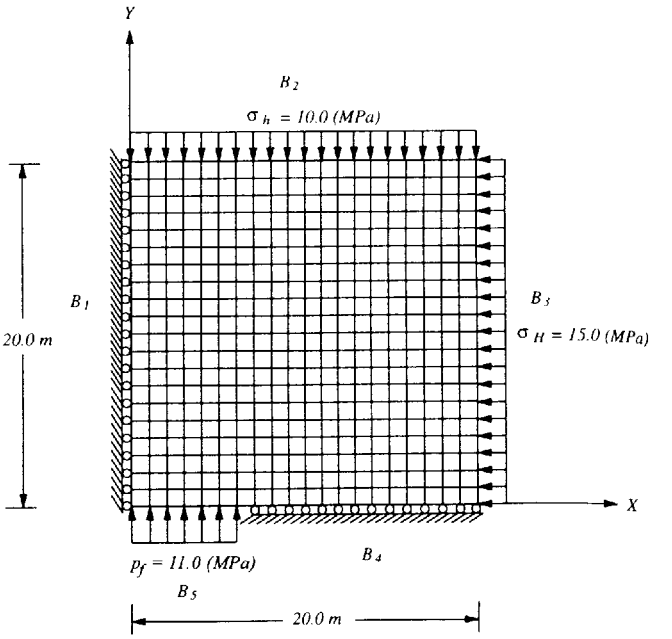

FIG. 3. The mesh and boundary conditions for the simulated problem. B1, a boundary that divides two symmetrical domains; B2, the far-field boundary that is parallel to the fracture and the minimum in situ stress is normal to this boundary; B3, the far-field boundary that is normal to the fracture and the maximum in situ stress is normal to this boundary; B4, a boundary that divides two symmetrical domains in the fracture tip region; B5, the hydraulic fracture on which the fracture pressure is applied.

Mohr–Coulomb criterion with a perfect plastic yield surface. It is assumed that before plastic yielding, the material is linear and elastic. Our finite element simulation shows that there is a nonnegligible discrepancy between the minimum in situ stress σ_h and the shut-in pressure p_s. Numerical results included in this paper qualitatively demonstrate the influence of the plastic zone on the shut-in pressure.

Both linear elastic fracture mechanics (LEFM) and nonlinear elastic fracture mechanics (NEFM) have been used to simulate a hydraulic fracture in the past. The LEFM theory produces a singularity near the fracture tip, whereas the NEFM, even though it avoids the infinitely high stress concentration on the tip, may not be used to predict accurately the stress profile in the so-called process zone. The fracturing fluid is assumed not to reach the fracture tip, so a fluid lag zone may exist, and the stress distribution in this fluid lag zone has been assumed to be equal to the minimum in situ stress normal to the fracture plus the rock tensile strength (Boone 1989; Papanastasiou and Thiercelin 1993; Van Den Hoek et al. 1993).

The classical fracture mechanics has been used extensively to deal with elastoplastic deformation near the fracture tip (Drugan et al. 1982; Castaneda 1987), and the materials under consideration have been treated as a Tresca media. Recently, coupled elastoplastic models have been used to simulate hydraulic fracture (Papanastasiou and Thiercelin 1993; Van Den Hoek et al. 1993). They studied both the fracturing pressure in response to an active loading and the geometrical change of a fracture due to the elastoplastic behavior. Because shut-in is an unloading process, in this article both loading and unloading processes will be simulated. The impact of such loading–unloading on the

TABLE 1. Input parameters

Young's modulus E (MPa)	Poisson's ratio ν	Frictional angle ϕ_p (°)	Cohesion strength c (MPa)	Tensile strength T_0 (MPa)	Dilatant angle ϕ_d (°)
10 000	0.25	30	0.3	0.0	30

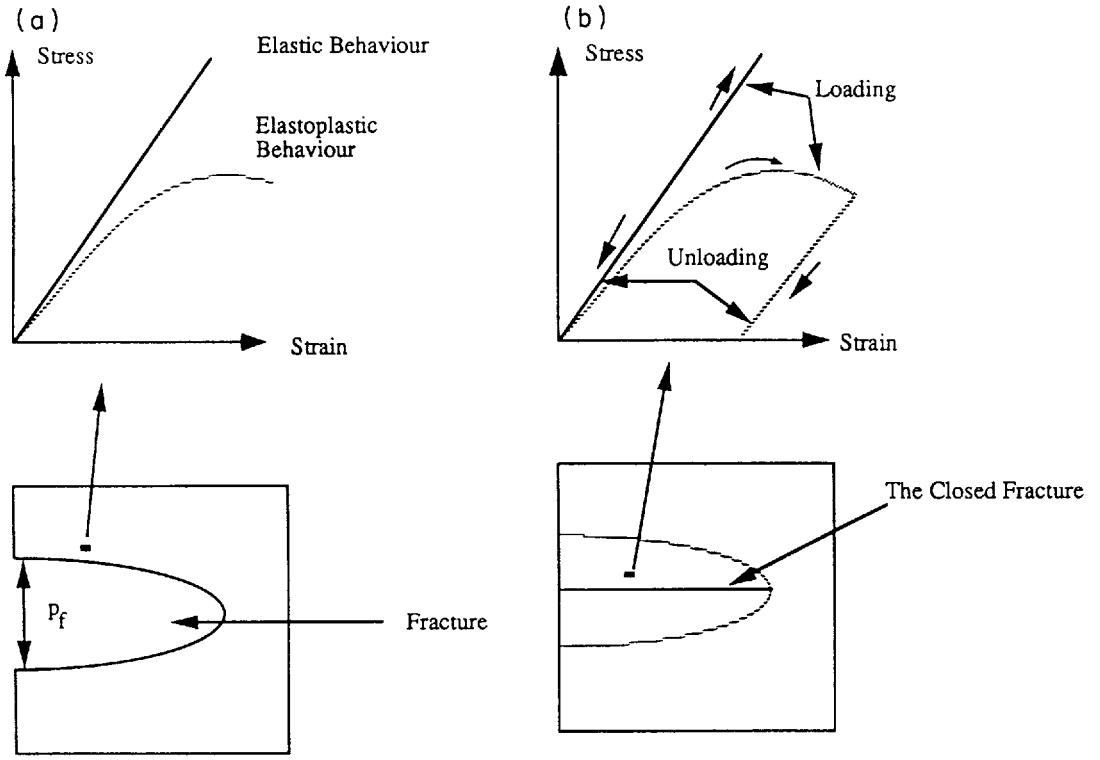

FIG. 4. A schematic diagram of loading and unloading near a fracture. (*a*) Active fracturing. The bottom diagram shows the opened fracture, and the top diagram shows the stress–strain responses of the material near the fracture for both pure elastic and elastoplastic models. (*b*) Fracture closure. The broken lines in the bottom diagram show the trajectory of the previously opened fracture. The top diagram shows the unloading trajectory after a plastic yielding state has been reached.

minimum in situ stress measurement is analyzed. For simplicity, a continuum mechanics is employed.

To demonstrate the processes of fracturing and the induced plastic zone, a specific loading path from a typical field test is taken (Fig. 1). The complete stress field consists of an existing stress field due to loading and another stress field due to unloading that simulates a shut-in process.

The paper is outlined as follows. First, both the geometry and the material properties of the fracturing model are described. The assumptions used in this paper are listed and discussed. Then the numerical results are presented, and the fracturing pressure p_s, corresponding to the fracture closure, is compared with the far-field stress σ_h. The discrepancy between p_s and σ_h is discussed finally and some conclusions are made.

Description of the model, assumptions, and boundary conditions

Governing equations

For elastoplastic media, the general form of constitutive equations in incremental form, in terms of stress and strain tensors (i.e., $d\sigma_{ij}$ and $d\epsilon_{kl}$), is written as follows:

$$[3]\quad \mathbf{d}\sigma_{ij} = D^{ep}_{ijkl}\,\mathbf{d}\epsilon_{kl}$$

where D^{ep}_{ijkl} is the elastoplastic stiffness matrix, and

$$[4]\quad \mathbf{d}\epsilon_{kl} = \mathbf{d}\epsilon^{e}_{kl} + \mathbf{d}\epsilon^{p}_{kl}$$

The superscripts e and p represent the elastic and plastic components, respectively. For Mohr–Coulomb materials, the yield function F, which separates elastic and plastic states, may be expressed by

$$[5]\quad F = \frac{\sigma_1 + \sigma_3}{2}\sin(\phi_p) - \frac{\sigma_1 - \sigma_3}{2} - c\cos(\phi_p)$$

where σ_1 and σ_3 are maximum and minimum principal stresses, respectively; ϕ_p is the peak frictional angle; and c is the cohesion.

Description of the problem

Like the conventional simulation on hydraulic fracturing, the fracture simulated in this paper is assumed to be static and the fracture shape is rectangular. The material adjacent to the fracture is assumed to be isotropic and homogeneous, and a two-dimensional plane-strain condition is assumed. Only one quarter of the complete domain surrounding the fracture needs consideration in the numerical analysis due to symmetry (see Fig. 2). The finite-element (FE) mesh used and boundary conditions for the problem are described in Fig. 3.

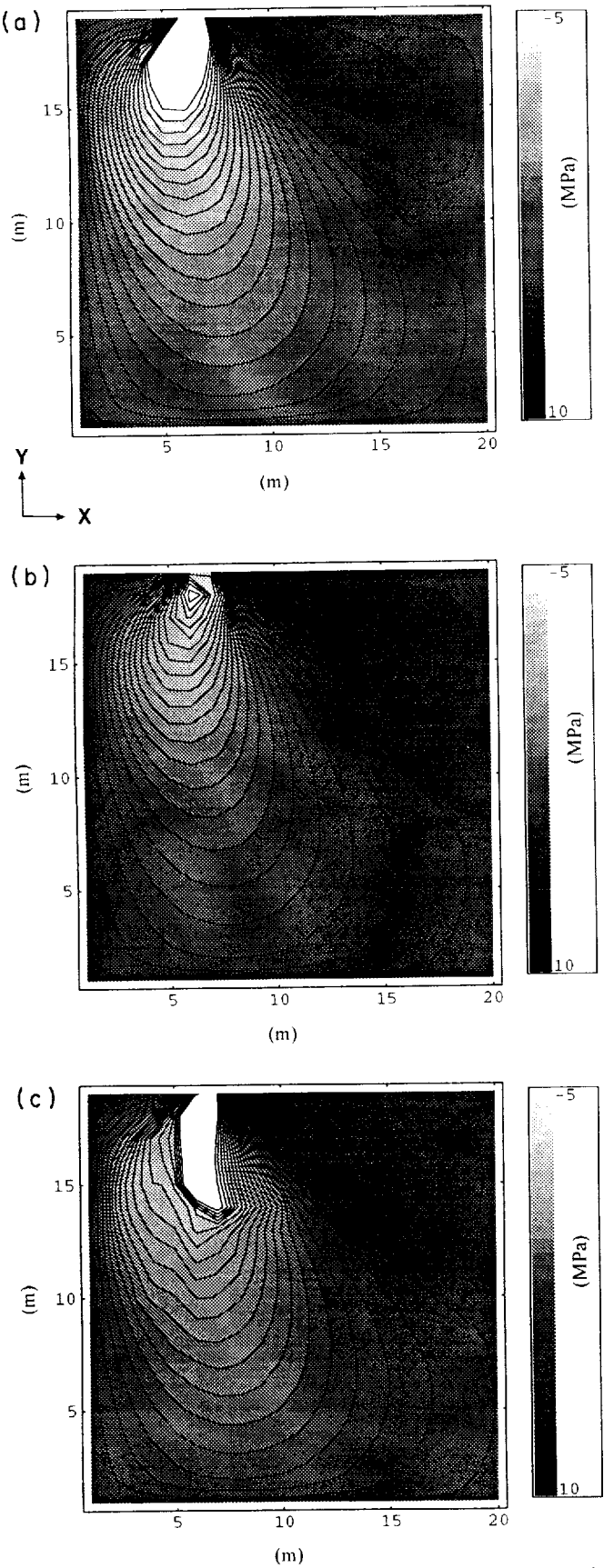

FIG. 5. Shear-stress evolution near a fracture during active loading and unloading. (*a*) Loading step 41 in our numerical simulation, in with σ_h = 8 MPa, σ_H = 12 MPa, and P_f = 8.8 MPa. Those figures before this loading step are not displayed because no shear-stress pattern change can be observed up to this loading stage. A fracture pressure to the normal stress ratio p_f/σ_h of 1.1 has been maintained. (*b*) Loading step 53 when the fracture pressure to normal stress ratio p_f/σ_h is increased to 1.35. More significant shear-stress concentration may be observed at the fracture tip. (*c*) Shows an unloading repsonse taking place inside the fracture. One may observe the reduction in shear stress at the fracture tip.

There are 400 isoparametric elements and 448 nodes used in the simulations.

To simulate the loading inside the fracture, loading is imposed on boundaries B2, B3, and B5 simultaneously, and displacement in the x direction for B1 and the y direction for B4 is kept fixed. The loading on B5 is slightly larger than those on B2 and B3, since a larger pressure is needed inside the fracture to make the fracture open farther. Because a breakdown pressure that is 15% higher than the far-field stress may be required for some typical rocks (Boone 1989), in our numerical simulations, an additional 10% pressure is added on the surface of the fracture. This additional 10% fracturing pressure is reduced to zero at the end of the unloading that simulates the shut-in process for stress estimate.

Major assumptions

A hydraulic fracturing process may be completed in a few minutes. Such a short injection period may only allow a limited amount of fluid from the open fracture to penetrate into the matrix formation adjacent to the fracture. Also, an intact oil sand has a permeability about 0.1–10 MD (10^{-12} cm/s) (Boone et al. 1991*a*). Thus, the poroelastic effect may be limited to a small region near the fracture and the possible error induced by this impermeability is assumed negligible, in comparison to the plastic effect.

A static fracture is assumed in this paper to represent a *snapshot* of a moving fracture. This kind of method may not rigorously represent the dynamic process of a fracture propagation, but it has been widely used in petroleum engineering and rock mechanics studies (Haimson and Fairhurst 1969; Dusseault and Simmons 1982). The stress state corresponding to this static fracture is calculated by a combination of two stress states: one corresponding to a stage when the fracture stops propagating, and the other corresponding to the process between the end of the former state and the state when the fracture is completely closed. The separating point between the two states has been defined as the breakdown, where the maximum bottom-hole pressure may be defined.

An elastic and perfectly plastic model is used as the first attempt in our analysis simulating the poorly consolidated materials (Florence and Schwer 1978; Bratli and Risnes 1981; Senseny et al. 1989). At this time, neither the poroelastic nor the thermal effects are considered, as only a low-permeability material is of interest in our simulation.

The material properties used here are taken from Dusseault (1977) and Dusseault et al. (1988) for oil sands (Table 1). The boundary conditions are chosen such that a reservoir in about 1 km depth may be simulated.

Even though there are some analytic solutions to the problem of a propagating fracture in poroelastic media (Haimson and Fairhurst 1969), it appears difficult to solve our problem analytically due to the nonlinearity. Numerical methods thus must be employed (Smith 1982; Boone 1989). It turns out that the finite element method (FEM) is effective in solving

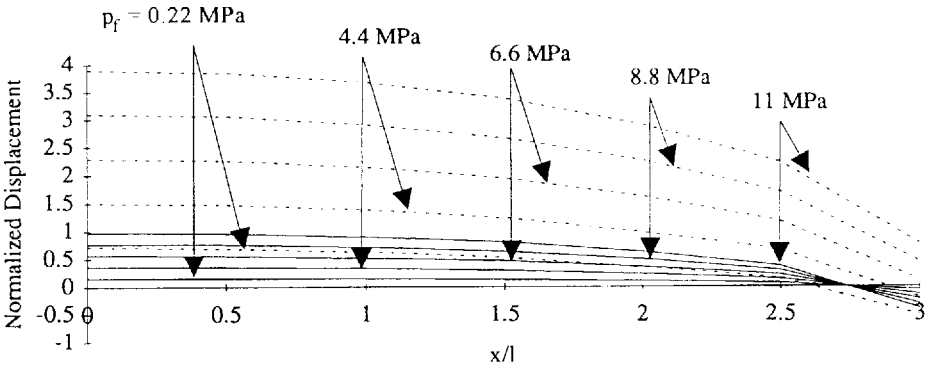

FIG. 6. The displacements near a fracture for both loading and unloading. The broken and the solid lines denote the loading and unloading responses, respectively. All displacements shown in the figure are normalized by the maximum displacement at each element when the fracture pressure is equal to 11 MPa for the active loading case. l and x, fracture length and distance away from the fracture mouth in the direction parallel to the fracture, respectively.

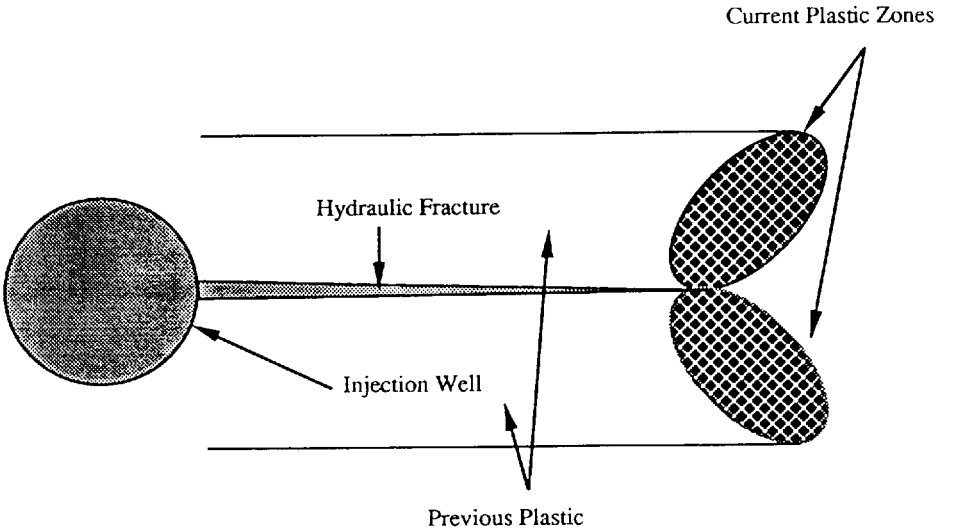

FIG. 7. A schematic diagram of the plastic zones near a fracture.

this nonlinear problem. The initial stress method is employed for the finite-element formulation, and a code based on the subroutine provided by Smith (1982) is used. Both the loading paths and numerical results obtained by the FEM are described in the next section.

Summary of the problem

In hard rocks such as granite, marble, and some limestones, it is conceivable that the concentration of shear stress near the fracture tip may be limited to a small region. Hence, most of the induced deformation near the fracture is elastic and can be reversed after the pressure inside the fracture is reduced. For soft rocks such as clay and oil sands, it is not clear whether the deformation near a fracture is reversible once the injection pressure is shut off. Even if the deformation ultimately decays to zero, the shut-in pressure may not correspond to the far-field minimum stress because the loading and unloading follow different stress paths, i.e., different strains or displacements on the fracture face may correspond to the same stress field (Fig. 4). Hence a hysteresis in the stress–strain response must be considered and the existing elastic theory for stress measurement by hydraulic fracture becomes questionable.

To understand the process of a fracture propagation and the shut-in response in a poorly consolidated medium, it is essential to qualitatively describe this hysteresis response according to the stress evolution. The FEM is used to simulate the evolution of a fracture and the poorly consolidated medium is assumed to be elastic and perfectly plastic after yielding. Using this model, a plastic zone can be generated adjacent to the hydraulic fracture. The shear-stress evolution, which contributes to the plastic-zone propagation, is analyzed.

Numerical results and discussion

In Fig. 5, the shear-stress evolution near the fracture tip during pressurization of the fracture is shown. The fracture is located on the top left corner; the nonshaded and the completely shaded regions represent the maximum shear stress of two opposite modes, respectively, (i.e., the positive and negative shear stresses). A positive shear stress contributes to generating an active plastic zone (such a pattern will be shown later in Fig. 9), whereas the negative shear stress may reduce the shear stress due to the previously concentrated stresses (i.e., the stresses due to a bypassing fracture). Figure 5*a* shows the shear stress contour plot in the neighborhood of the fracture, which is located at the upper left corner with a length of 7 m. This stress-contour plot corresponds to a stress ratio p_f/σ_h of 1.1, where p_f is the current fracture pressure. It is worth emphasizing that the stress contour remains the same as long as the ratio is

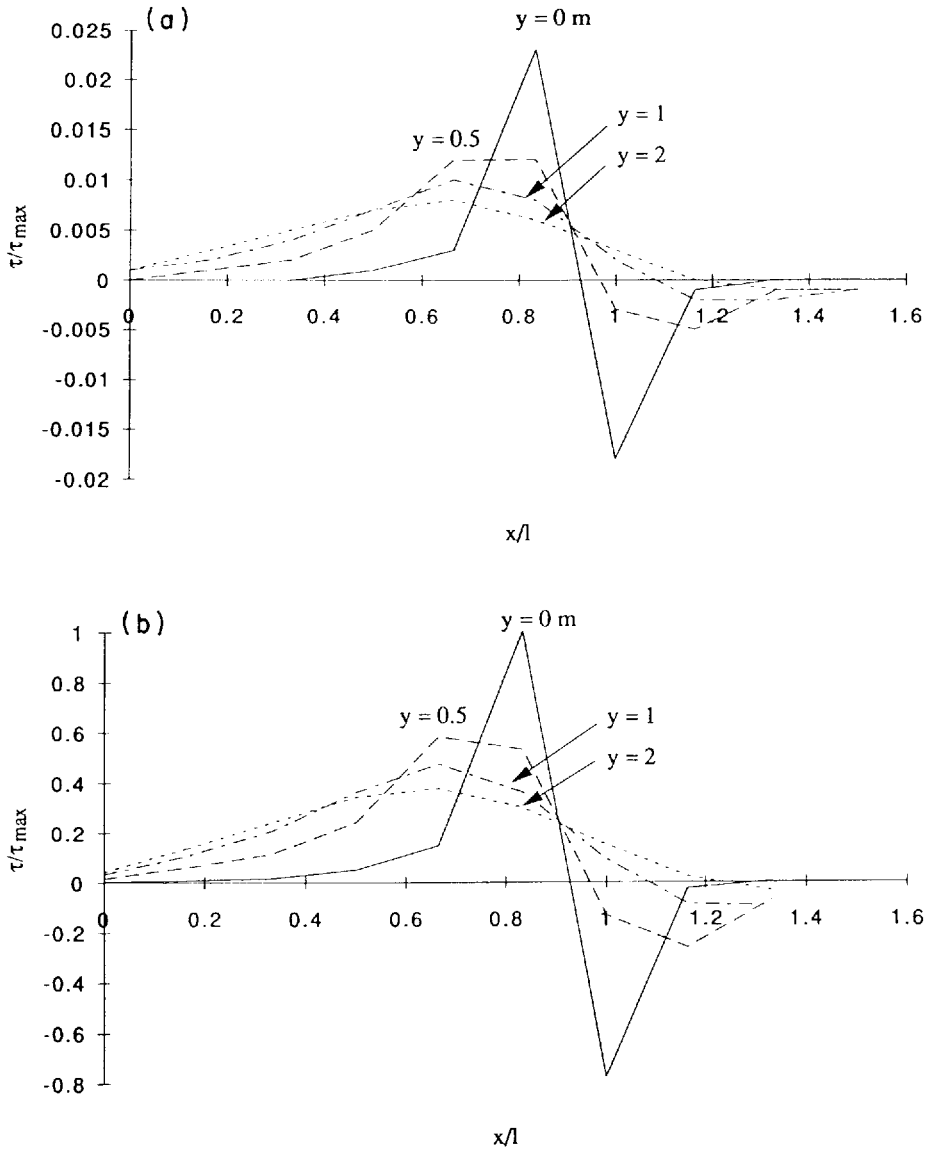

FIG. 8. Shear stresses near the fracture surface. (a) Low-stress case. Fracture pressure = 0.22 MPa. (b) High-stress case. Fracture pressure = 11 MPa. In both cases, the shear stress τ is normalized by the maximum shear stress τ_{max}, which is obtained for the maximum fracture pressure of 11 MPa. l, fracture length; x and y, distance away from the fracture mouth in the direction parallel to and normal to the fracture, respectively.

kept unchanged, even though both the fracture pressure p_f and the normal in situ stress σ_h may increase. As the fracture pressure p_f increases, which results in an increase of the ratio p_f/σ_h, the negative shear stress region is reduced. But the positive shear stress may accumulate on the tip of the fracture, around which a larger plastic zone may be produced (Fig. 5*b*). Conversely, as the fracture pressure p_f decreases to simulate the shut-in process, the negative shear stress region may increase. This leads to a stress relaxation at the fracture tip (Fig. 5*c*). The range of the plastic zone generated during an active loading may not be reduced, even though the shear stresses in these yielded regions are reduced. This is because the plastic deformation is not reversible.

To demonstrate some effect of the plastic deformation on the shut-in pressure, the evolution of the displacement near the fracture, during the fracturing and closing processes is analyzed. Figure 6 shows the displacements under both loading and unloading, but with different fracture pressures for each pair of curves. For example, the displacement corresponding to the active loading of 8.8 MPa is achieved by inputting a fracture pressure of 8.8 MPa, and the corresponding unloading curve is obtained by unloading the pressure from 8.8 to 0 MPa from the fracture surface after the active loading. One may see that residual displacements exist around the elements adjacent to the fracture after the fracture pressures are completely unloaded. Such residual displacements become larger as the maximum fracture pressures increase (the maximum fracture pressure is 11 MPa in our case). Under the aforementioned conditions, it may be deduced that a hydraulic fracture may not be closed under a fracture pressure of 10 MPa, which corresponds to the far-field in situ stress in our case. Thus, a fracture pressure that is much smaller than the far-field stress may correspond to the fracture closure, and only in this way can the fracture be closed. This suggests that either the shut-in pressure does not correspond to fracture closure pressure or the shut-in pressure is much smaller than the far-field stress, if a plastic zone is generated near the fracture.

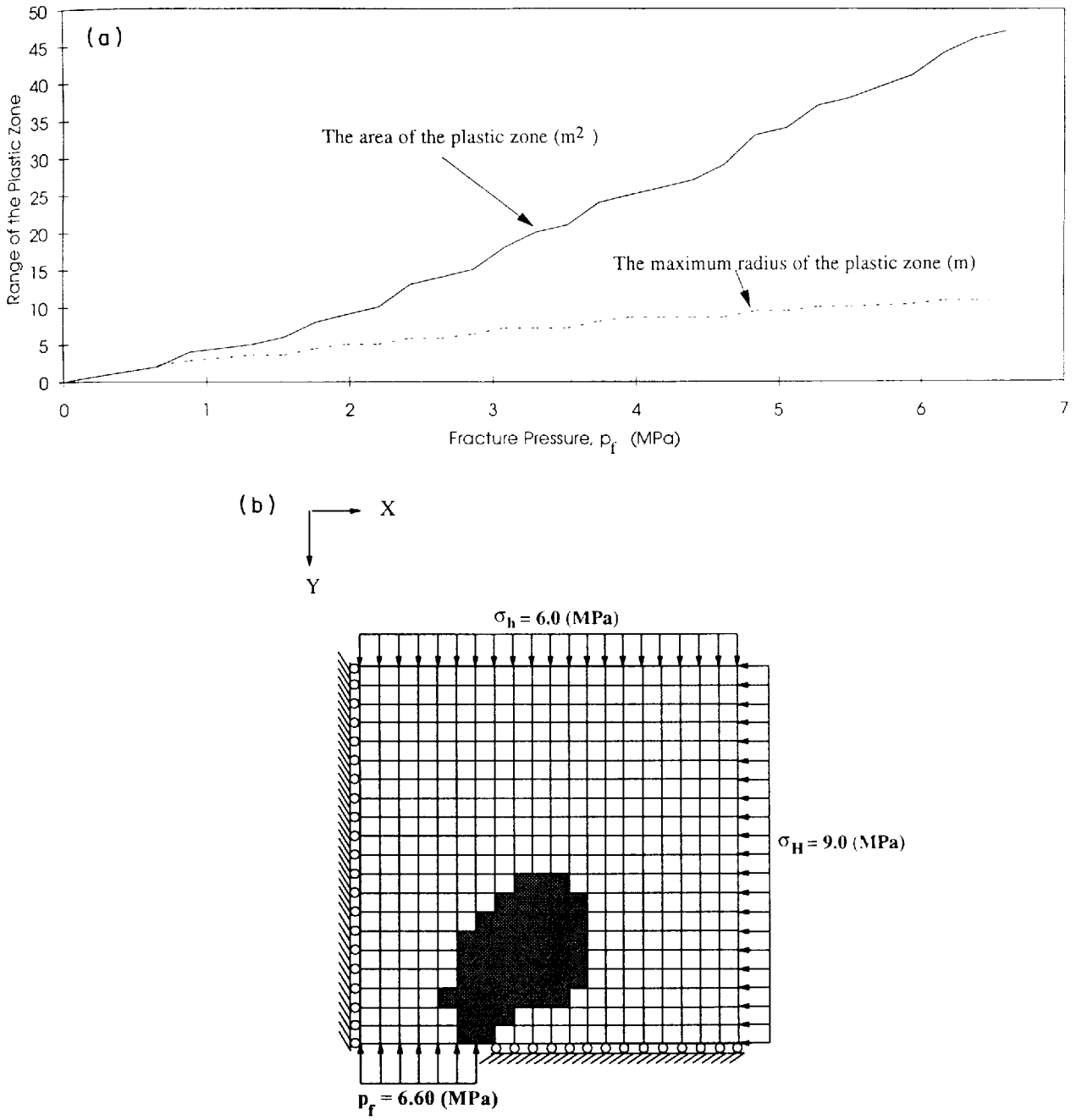

FIG. 9. Plastic zone evolution near the fracture during fracturing. (*a*) Fracture pressure vs. maximum plastic radius and plastic area. (*b*) A typical numerically calculated pattern of the plastic zone near the fracture. (Also, see Fig. 3 for the definition of the boundaries).

We would like to point out that only a static fracture is simulated and the plastic zone is localized near the fracture tip. The plastic yielding zone in practice may, however, sweep all the region behind the current plastic region. Figure 7 shows a *snapshot* schematic diagram of the plastic-zone propagation near a fracture. A more rigorous calculation of deformation should combine the preexisting deformation due to the effect of the passing-by fracture and the deformation due to the support fluid pressure inside the fracture after the fracture is opened. Only the latter is the main focus of this paper because the issue considered in this paper is to address the potential error caused by the irreversible deformation near the fracture, and the limitations of the conventional hydraulic stress measurement technique.

Figures 8*a* and 8*b* describe the calculated shear stress near a fracture. These two diagrams correspond to two different loading stages but have a similar stress pattern. This indicates that the ratio of the fracture pressure to the far-field minimum in situ stress controls the shear-stress pattern.

Finally, we show the plastic-zone propagation under different fracture pressures (Fig. 9). This is achieved by the following loading procedure: the vertical and right-lateral in situ stress and the pressure inside the fracture are imposed simultaneously at an increment of 2% of the total loading. An initial plastic yielding is produced at step 3 when the fracture pressure is 0.66 MPa, the lateral stress is 0.9 MPa, and the vertical stress is 0.6 MPa. The plastic zone starts from the fracture tip and propagates into the formation as the fracture

pressure increases. Only those results up to 50% of the maximum fracture pressure (i.e., less than 7 MPa) are presented in this figure, as there is no major difference in the trend of the plastic-zone evolution for higher fracture pressures. A frictional angle of 30° has been used to simulate this process, despite a peak frictional angle of 42° being previously reported for oil sands (Dusseault 1977). Such a small frictional angle was chosen because the peak frictional angle only reflects the peak strength, below which a plastic yielding has already occurred. In other words, a plastic yielding appears much earlier than the peak strength. Figure 9*b* shows the typical outline of a plastic zone, in which the fracture is located at the left corner, the lateral maximum in situ stress σ_H = 8.7 MPa, the normal minimum in situ stress σ_h = 5.8 MPa, and the fracture pressure p_f = 6.38 MPa.

Concluding remarks

A simple FEM has been used to simulate the stress evolution near a static fracture during the process of hydraulic fracturing and shut-in. A plastic zone is usually generated near the fracture in a poorly consolidated medium and irreversible deformation may appear during the fracturing process. Shut-in is a process of unloading with respect to the active fracturing (i.e., loading) process. This unloading must be considered as an incremental process, and the stresses due to this process may be added to the preexisting stress field. Because of the irreversible deformation adjacent to the fracture, the fracture closure pressure is much smaller than the far-field stress normal to the fracture plane. If the shut-in pressure corresponding to the fracture closure pressure is used for the estimate of minimum in situ stress, a large error may be introduced. The reason is that the conventional hydraulic fracturing technique is founded on elasticity theory, but an additional normal stress in the minimum in situ stress direction is required to close the fracture after a plastic zone is generated near the fracture. To reduce such an error due to the plastic deformation near the fracture, the breakdown pressure may be reduced so that the plastic zone surrounding the fracture is kept minimal. This may be achieved by using a less viscous injection fluid. A less viscous fluid, however, may increase the poroelastic effect that may also increase the breakdown pressure by about 30% (Boone 1989). This again may induce an error for the stress measurement by the conventional technique. An alternative is to conduct a rapid injection by a less viscous fluid. Again, a higher breakdown pressure may be found for a high injection rate because of a possible dynamic effect and less diffusion (Haimson and Fairhurst 1969). It seems that a higher breakdown pressure is unavoidable, caused by either a poroelastic effect or a dynamic response. Such a higher breakdown pressure, as demonstrated in this paper, may lead to erroneous information regarding the far-field minimum stress. It is suggested that an optimized design for injection, taking all the factors mentioned above into account, may be essential for a successful operation to obtain accurate information of the in situ stresses. The results presented here are applicable to those weak rocks such as oil sands and clay. Further study will be conducted for more advanced constitutive models including the poroelastoplastic model to improve qualitative prediction of the error. The constitutive modelling itself warrants a full-scale research effort.

In conclusion, a large plastic zone may be induced near a hydraulic fracture in poorly consolidated rocks such as oil sands and clay. Irreversible deformation may be induced near the fracture after the fracture pressure reduces to a level that is equal to the far-field normal stress. The fracture closure pressure in such plastically yielded rocks can be much smaller than the far-field stress normal to the fracture. Thus, the conventional in situ stress measurement technique by hydraulic fracturing may produce erroneous data in these aforementioned rocks. One must take this factor into account when a hydraulic test is conducted in a poorly consolidated medium.

Acknowledgments

This work was supported in part by Energy, Mines and Resources Canada and the Natural Sciences and Engineering Research Council of Canada. The first author would like to express his deep gratitude to Dr. J.D. Scott of the University of Alberta for his financial support of this work.

Boone, T.J. 1989. Simulation and visualization of hydraulic fracture propagation in poroelastic rock. Ph.D. thesis, Cornell University, Ithaca, N.Y.

Boone, T.J., Kry, P.R., Bharatha, S., and Gronseth, J.M. 1991*a*. Poroelastic effects related to stress determination by microfrac tests in permeable rock. *In* Rock Mechanics as a Multidisciplinary Science, Proceeding of the 33rd U.S. Symposium on Rock Mechanics, July 10–12, Norman, Okla. *Edited by* J.-C. Roegiers, A.A. Balkema, Rotterdam, The Netherlands, pp. 25–34.

Boone, T.J., Ingraffea, A.R., and Roegiers, J.-C. 1991*b*. Simulation of hydraulic fracture propagation in poroelastic rock with application to stress measurement techniques. International Journal of Rock Mechanics and Mining Sciences and Geomechanics Abstracts, **28**: 1–14.

Bratli, R.K., and Risnes, R. 1981. Stability and failure of sand arches. Society of Petroleum Engineers Journal, **21**: 236–248.

Castaneda, P.P. 1987. Plastic stress intensity factors in steady crack growth. Journal of Applied Mechanics, **54**: 379–387.

Detournay, E. 1987. Elastoplastic model of a deep tunnel for a rock with variable dilatancy. Rock Mechanics and Rock Engineering, **19**(2): 99–108.

Drugan, W.J., Rice, J.R., and Sham, T.L. 1982. Asymptotic analysis of growing plane strain tensile cracks in elastic – ideally plastic solids. Journal of the Mechanics and Physics of Solids, **30**: 447–473.

Dusseault, M.B. 1977. The geotechnical characteristics of Athabasca oil sands. Ph.D. thesis, The University of Alberta, Edmonton.

Dusseault, M.B., and Simmons, J.V. 1982. Injection-induced stress and fracture orientation changes. Canadian Geotechnical Journal, **21**: 48–56.

Dusseault, M.B., Wang, Y., and Simmons, J.V. 1988. Induced stresses near a fireflood front. Alberta Oil Sands Technology and Research Authority: Journal of Research, **4**: 153–170.

Florence, A.L., and Schwer, L.E. 1978. Axisymmetric compression of a Mohr–Coulomb medium around a circular hole. International Journal for Numerical and Analytical Methods in Geomechanics, **2**(4): 367–379.

Gronseth, J.M., and Kry, P.R. 1983. Instantaneous shut-in pressure and its relationship to the minimum in-situ stress. *In* Hydraulic Fracturing Stress Measurement. *Edited by* M.D. Zoback and B.C. Haimson. National Academic Press, Washington, D.C. pp. 55–60.

Haimson, B., and Fairhurst, C. 1969. In-situ stress determination at great depth by means of hydraulic fracturing. *In* Theory and Practice. *Edited by* W.H. Somerton. Society of Mining Engineers, Berkeley, Calif. pp. 559–584.

Hubbert, M.K., and Willis, D.G. 1957. Mechanics of hydraulic fracturing, Transactions of American Institute of Mining, Metallurgical, and Petroleum Engineers, **210**: 153–166.

Nolte, K.G. 1979. Determination of fracture parameters from fracture pressure decline. *In* Proceeding of the 54th Annual Technical Conference and Exhibition of the Society of Petroleum Engineering (SPE8341), Las Vegas, Nev. pp. 21–36.

Papanastasiou, P., and Thiercelin, M. 1993. Influence of inelastic rock behaviour in hydraulic fracturing. International Journal of Rock Mechanics and Mining Sciences and Geomechanics Abstracts, **30**: 1241–1247.

Schmitt, D.R., and Zoback, M.D. 1989. Poroelastic effects in the determination of the maximum horizontal principal stress in hydraulic fracturing tests—a proposed breakdown equation employing a modified effective stress relation for tensile failure. International Journal of Rock Mechanics and Mining Sciences and Geomechanics Abstracts, **26**: 499–506.

Senseny, P.E., Lindberg, H.E., and Schwer, L.E. 1989. Elastic–plastic response of a circular hole to repeated loading. International Journal for Numerical and Analytical Methods in Geomechanics, **13**: 459–476.

Smith, I.M. 1982. Programming the finite element method—with application to geomechanics. John Wiley & Sons, Inc., New York.

Van Den Hock, P.J., Van Den Berg, J.T.M., and Shlyapobersky, J. 1993. Theoretical and experimental investigation of rock dilatancy near the tip of a propagating hydraulic fracture. International Journal of Rock Mechanics and Mining Sciences and Geomechanics Abstracts, **30**: 1261–1264.